Catalytic *n*-Butane Oxidation Activity and Physicochemical Characterization of Vanadium-Phosphorus Oxides with Variable P/V Ratio

F. GARBASSI,* J. C. J. BART,*,1 R. TASSINARI,* G. VLAIC,* AND P. LAGARDE†,1

*Istituto Guido Donegani S.p.A. (Montedison Group), Novara Research Center, Via G. Fauser 4, 28100 Novara, Italy; †Université de Paris-Sud, LURE, Orsay Cédex, France

Several (V,P)O catalysts (with atomic ratio P/V from 0.93 to 1.28) for oxidation of *n*-butane to maleic anhydride were examined by means of bulk (XRD and EXAFS) and surface (XPS) techniques in relation to their activity. A correlation was observed between the onset of the oxidation of vanadium in dried catalysts upon calcination and the value of the surface P/V ratio. The specific conversion increases by an order of magnitude for a P/V ratio just exceeding unity. The slight excess of phosphorus with respect to 1 : 1 stoichiometry stands in relation to a delay in oxidation rate of V(IV). EXAFS results suggest that excess phosphorus does not induce structural effects. © 1986 Academic Press, Inc.

INTRODUCTION

Synthesis of maleic anhydride through C_4 hydrocarbon (*n*-butane or butene-1) oxidation is a chemical process which has enjoyed wide interest in recent years (*1, 2*). Most catalysts for this reaction contain mainly vanadium and phosphorus in an oxidized form, in addition to other metal cations (*1*), which make the solid system difficult to study. As it turns out, even the binary (V,P)O system is already rather complicated because of the great variety of observed phases, both in the precursor state (depending strongly on the nature of the reducing agent used for preparation (*3–5*)) and after activation by calcination (*6, 7*).

In previous work oxidation during calcination of tetravalent vanadium in dried catalysts has been related to the P/V ratio (*7*). It is the purpose of this paper to examine this effect in greater detail by physicochemical characterization with bulk and surface techniques of a series of (V,P)O catalysts with an atomic ratio P/V centered around

unity, and to relate the observations to the catalytic activity.

EXPERIMENTAL

Catalyst preparation. Catalyst samples with P/V atomic ratios in the range 0.93 to 1.28 were prepared by adding the appropriate amount of aqueous H_3PO_4 to a blue solution formed by stirring V_2O_5 and HCl in water at room temperature for 4 h. After evaporation to dryness the pale green solids were treated at 423 K in air for 2 h.

Catalytic activity. For catalytic activity measurements a conventional stainless-steel flow reactor was loaded with about 2 g of the granulated catalyst and a feed of 1.5% *n*-butane in air was admitted at a spatial velocity of 5700 h⁻¹. A gas-chromatographic system was used to check the inlet gas mixture and to determine the conversion C, defined as

$$C = \frac{\text{moles of } n\text{-butane consumed}}{\text{moles of } n\text{-butane fed}} \times 100.$$

The measurements were carried out in the temperature range 573 to 673 K using samples previously heated in air at 673 K for 4 h

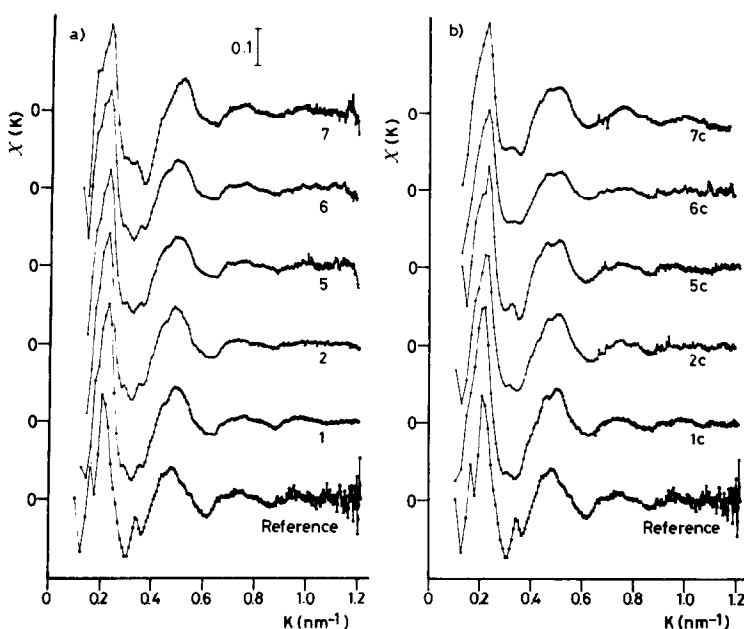1 Present address: Central Laab DSM, P.O. Box 18, Geleen, Nederland.

317

FIG. 1. EXAFS P K-edge spectra of (a) $NH_4H_2PO_4$ and dried (V,P)O catalysts; (b) calcined (V,P)O catalysts.

and cooled to 573 K prior to the catalytic runs.

Physicochemical characterization. Chemical analysis has been carried out by standard methods (5). Specific BET surface area (SSA) values at liquid-nitrogen temperature were measured with a Carlo Erba Sorptomatic system and XRD patterns were taken on a Philips PW 1050 powder diffractometer using Cu $K\alpha$ radiation.

Samples for EXAFS measurements were prepared by suspending ultrasonically 5 mg of each sample in 25 cm^3 of dry n-heptane, and adding some drops of dry Vaseline. The suspensions were filtered on 10-μm-thick Nucleopore membranes ($\phi = 1.5$ cm) and the loaded membranes were checked optically (at 140×) for the absence of fractures and for thickness uniformity. X-Ray absorption measurements of samples dried at 423 K and calcined at 723 K were carried out on the A42 line of the ACO storage ring (Orsay, France), with $E = 536$ MeV and $I = 150$ mA and a monochromator consisting of two parallel Ge(111) crystals. The speci-

mens were mounted on a suitable sample holder in a chamber pumped at 10^{-6} Torr, measuring the incident radiation I_0 and the transmitted radiation I_1 separately, by means of ionization chambers.

EXAFS P K-edge spectra at room temperature (Figs. 1a and b) were taken with $\Delta E = 2$ eV in the energy range 2000 to 2700 eV, recording I_1 and I_0 10 and 6 times, respectively. Threshold spectra were recorded within the 2130–2170 eV range, using $\Delta E = 0.3$ eV and a measuring time of 2 s per data point. Data analysis involved background removal by applying a Victoreen fit (8) and the absorption $\mu_0 X$ of the absorber without backscattering interference has been approximated by a fourth-order polynomial function. Spurious residual slow oscillations were eliminated, if any, by a multiiterative process. The photoelectron binding energy E_0 was initially taken at the inflection point of the K-edge and further treated as an independent parameter in the fitting procedure. Fourier transformation was carried out in the 2.5–
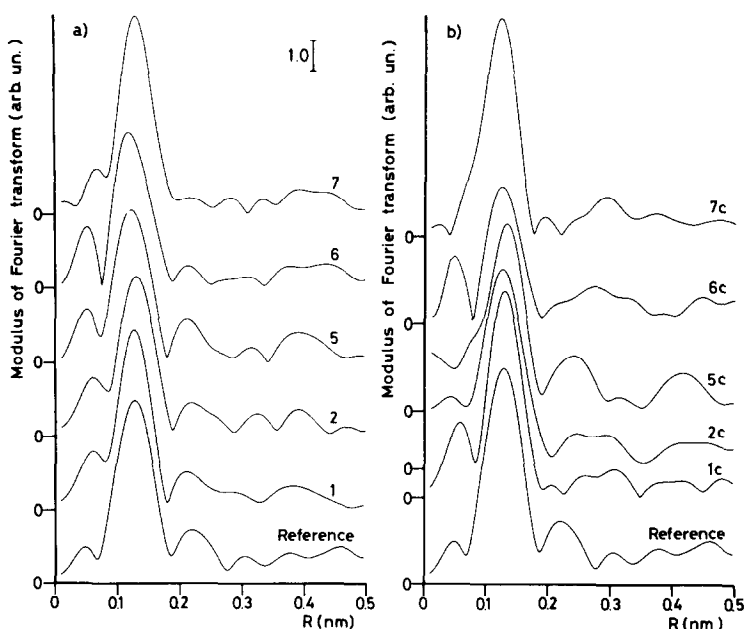
FIG. 2. Modulus of Fourier transform of P K-edge EXAFS spectra between $k_{min} = 2.5$ Å^{-1} and $k_{max} =$ 11.5 Å^{-1} of (a) $NH_4H_2PO_4$ and dried (V,P)O catalysts; (b) calcined (V,P)O catalysts.

11.5 Å^{-1} range with a Gaussian window function for damping the signal at values close to the integration limits. Figures 2a and b report the Fourier transform modules for dried and calcined samples, respectively. Structural parameters (coordination number N, coordination shell radius R, and Debye–Waller factor σ) were obtained in k-space (4–9 Å^{-1}) by fitting the Fourier-filtered spectra in a limited region of R space (Figs. 3a and b) using $NH_4H_2PO_4$ as a reference for computing phase and amplitude functions. Further details on spectral data acquisition and EXAFS signal analysis are reported elsewhere (9).

XPS has been performed on a PHI Model 548 system connected to a PDP 11/50 computer for data collection. $MgK\alpha$ radiation at 1253.6 eV has been used for exciting powder specimens inserted in a pure In foil; a flood electron gun minimized the electrostatic sample charging. Binding energies have been referred to the C $1s$ contamination peak at 284.6 eV. The intensities of O $1s$, V $2p$, P $2p$, and C $1s$ peaks were recorded, smoothed and measured after

background subtraction. The elemental sensitivity factor method has been used for determining the surface compositions (10).

RESULTS

Catalytic activity measurements (Table 1) show gradually increasing conversions toward higher reaction temperatures. After a delay of several hours at 673 K, the conversion drops in all cases. The discontinuous behavior of the conversion as a func-

TABLE 1

Conversion (%) for n-Butane Oxidation at Different Temperatures on (V,P)O Catalysts

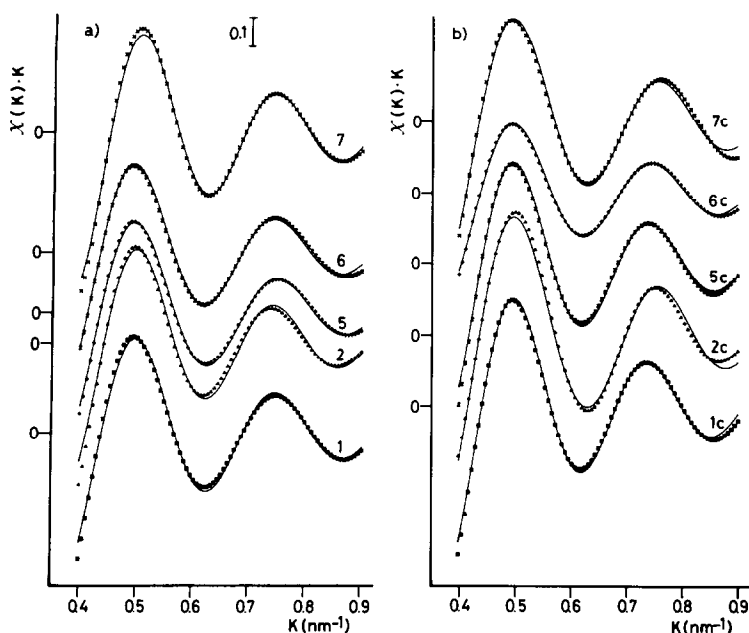| Sample	Conversion (%)			
	573 K	623 K	673 K (Initial)	673 K (3 h)
1	1.2	1.3	12.0	4.2
2	0.8	1.3	11.0	3.5
3	14.0	15.3	32.3	9.6
5	7.2	11.6	12.2	5.5
6	11.0	12.5	15.9	8.6
7	6.9	10.6	21.6	11.1

FIG. 3. Fit of $\phi_1(k,R)$ vs k function for P–O distances in the range 4–9 Å^{-1} for (a) dried (V,P)O catalysts; (b) calcined (V,P)O catalysts.

tion of the P/V ratio is rather interesting. Values obtained at 623 K are reported in Fig. 4. Very low conversion values are observed for $(P/V)_b < 1$ and an order of magnitude higher for $(P/V)_b > 1$ though with a slight decrease toward even higher phosphorus contents. Such a trend is consistent
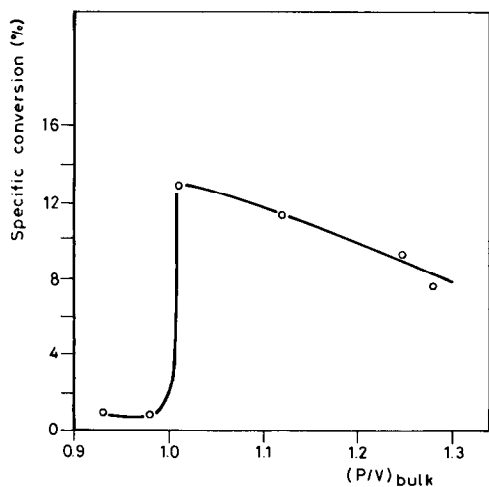

FIG. 4. Total n-butane conversion at 623 K as a function of $(P/V)_b$.

with results reported for the oxidation of butane (7) and butene-1 (3).

Chemical analysis of dried catalysts (Table 2) shows that all samples contain mainly V(IV), with small residues of V(V). According to XRD data (Table 3) all samples are composed of the precursor of the active β phase (11), though in the presence of small amounts of an unidentified phase. The X-ray spectral characteristics $(d(\text{Å}), I/I_0)$ of this unknown compound are: 7.02 vs, 6.86 mw, 6.70 w, 3.51 w, 3.05 w. Samples containing a marked excess of phosphorus contain also small quantities of $VO(H_2PO_4)_2$ (12). XRD results for catalyst samples discharged from the reactor show that those with $(P/V)_b > 1$ are generally more prone to changes than the others (Table 3). New phases are detected, such as β (11), $VO(PO_3)_2$ (13), and a phase observed at $P/V = 1.3$ (14). Generally speaking, $VO(H_2PO_4)_2$ is not affected by calcination and catalytic reaction. A further unidentified phase (y) has occasionally been observed in small amounts (characteristic d-spacings: 4.90, 4.24, 4.17, and 3.92 Å).

TABLE 2

Chemical Analysis, Specific Surface Area (SSA), and Surface Composition of Dried (V,P)O Catalysts

Sample	Chemical analysis (at.%)				SSA $(m^2\ g^{-1})$	Surface composition (at.%)			
	P	V	P/V	V(IV)/V(tot)		O	P	V	P/V
1	16.3	28.9	0.93	0.89	1.95	76.1	12.6	11.3	1.12
2	17.0	28.6	0.98	0.95	1.46	74.0	14.9	11.1	1.34
3	17.2	28.0	1.01	0.93	1.90	73.3	17.5	9.2	1.90
4	17.5	28.3	1.02	0.96	1.92	73.4	17.5	9.1	1.92
5	18.2	26.8	1.12	0.90	1.14	74.5	18.2	7.3	2.49
6	19.4	25.5	1.25	0.98	2.10	74.8	17.6	7.6	2.32
7	18.9	24.3	1.28	0.87	1.64	74.9	17.5	7.6	2.30

Parameters derived from EXAFS data analysis (N, R, and $\Delta\sigma^2$) by curve fitting are reported in Table 4 for both dried and calcined samples. Due to the narrow k range used for fitting (4–9 Å^{-1}), it is not possible to attribute a physical meaning to σ; only the difference with respect to the reference compound is meaningful. Estimated errors are 10–15% for N and $\Delta\sigma^2$ and 1–2% for R. An overall tetrahedral oxygen coordination around phosphorus is observed for all samples. In view of the complexity of the phase distribution (Table 3) such a coordination is apparently common to all component phases, with the exception of sample 7, where bond length contraction may just be significant. The observed P–O distances are very similar to

those of the reference compound. The disorder factor increases for higher $(P/V)_b$ ratios. Table 2 shows that the surface phosphorus-to-vanadium ratio $(P/V)_s$ is only directly proportional to the bulk ratio for $(P/V)_b < 1.1$. At higher values the surface ratio remains constant. The observed relationship between surface and bulk compositions for dried samples (Fig. 5) appears qualitatively similar to that found by other authors (7). Instead of the expected unitary value, the slope of the line for $(P/V)_b < 1$ approximates to 2, which is very near to

TABLE 3

Phases Detected by XRD in (V,P)O Catalysts after Drying at 423 K and after Catalytic Performance

Sample	Dried	Reactor discharged
1	d + h	d + h (s.a.)
2	d + h	x + h (s.a.) + y
3	d + h	d + h
4	d + h	Not measured
5	d + h + VO(H₂PO₄)₂	y + x + VO(PO₃)₂ + β
6	d + h + VO(H₂PO₄)₂	d + x + β + VO(H₂PO₄)₂ + y
7	d + h + VO(H₂PO₄)₂	d + x + y + VO(H₂PO₄)₂

Note. (s.a.) = small amount; d = precursor of phase β (*11*); x = phase detected by Morselli *et al.* (*14*); h, y = unidentified phases.

TABLE 4

EXAFS Data on Dried and Calcined (V,P)O Catalysts

Sample	N	R (Å)	$\Delta\sigma^2$ (Å²)	ΔE (eV)	E_0 (eV)
(NH₄)H₂PO₄ (Reference)	4.00(—)	1.53(—)	—	—	2141.7
1	4.20(0.5)	1.53(2)	0.0013	−6.6(1.0)	2143.0
2	4.35(0.5)	1.55(2)	0.0023	−7.5(1.0)	2142.7
5	4.35(0.5)	1.52(2)	0.0032	−4.9(2.0)	2142.3
6	4.25(0.5)	1.53(2)	0.0030	−6.6(1.0)	2142.3
7	4.50(0.5)	1.55(2)	0.0020	−9.0(1.0)	2142.7
1C[a]	4.10(0.5)	1.55(2)	0.0017	−8.0(1.0)	2142.7
2C	4.45(0.5)	1.52(2)	0.0016	−4.9(1.0)	2143.0
5C	4.05(0.5)	1.54(2)	0.0023	−8.0(1.0)	2142.4
6C	2.50(?)[b]	1.53(2)	?[b]	−6.0(1.0)	2142.7
7C	4.15(0.5)	1.49(2)	0.0024	0.0(1.0)	2142.7

[a] C: calcined.
[b] Results on samples 6C are affected by imperfect specimen preparation.
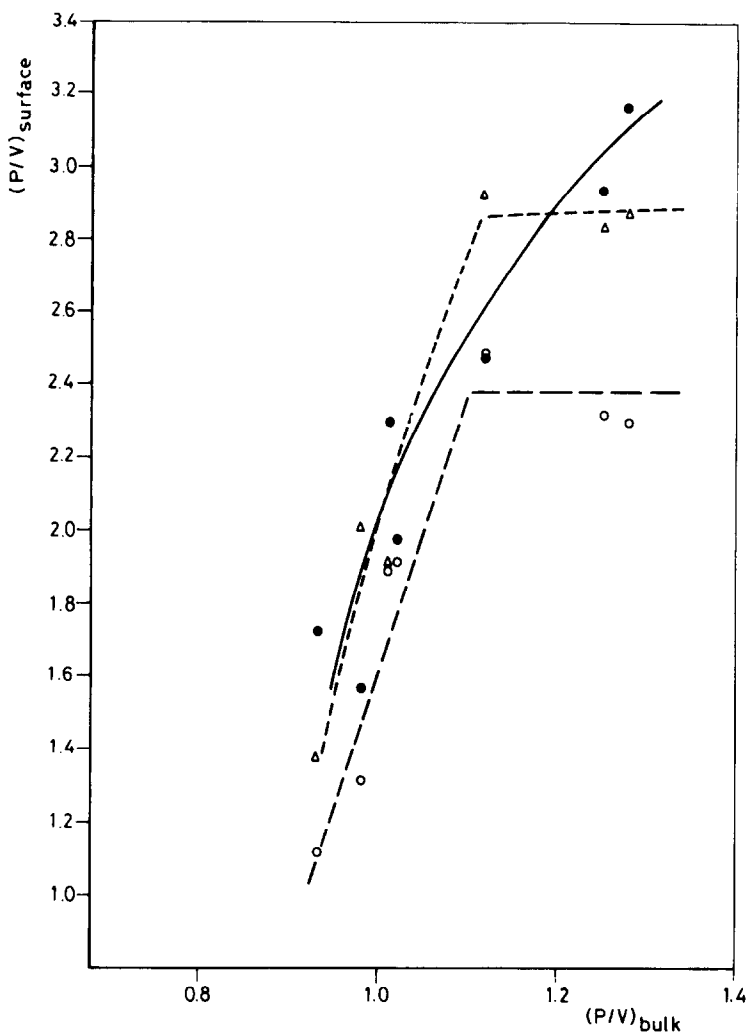
GARBASSI ET AL.

FIG. 5. Surface vs bulk V/P atomic ratios of catalysts after drying (O), calcination at 773 K (●), and reaction (△).

that found for another series of samples with a different phase composition (5). After heating the samples at 773 K, $(P/V)_s$ and $(P/V)_b$ are proportional in the whole range explored (Fig. 5); at the same time, $(P/V)_s$ ratios increase slightly also for bulk values below unity.

With increasing calcination temperatures the V $2p$ photoemission peaks undergo variations in shape and position on the energy scale, as shown in Fig. 6 for sample 3 in the O $1s$–V $2p$ region. On the other hand, the heating temperature has no effect on the P

$2p$ and O $1s$ peaks. Consequently, the plot of the energy differences between oxygen and vanadium peaks vs temperature clearly expresses the shift of the V $2p_{3/2}$ peak toward higher binding energies. Such variations (starting from a value of 516.0 eV up to 517.2 eV, with corresponding O–V separations of 14.2 and 13.0 eV, respectively) may be attributed to the oxidation of V(IV) to V(V). Figure 7 reports data for three samples with different $(P/V)_b$ ratios. The gradual changes in energy are caused by the prevalence of the V(IV) or V(V) component
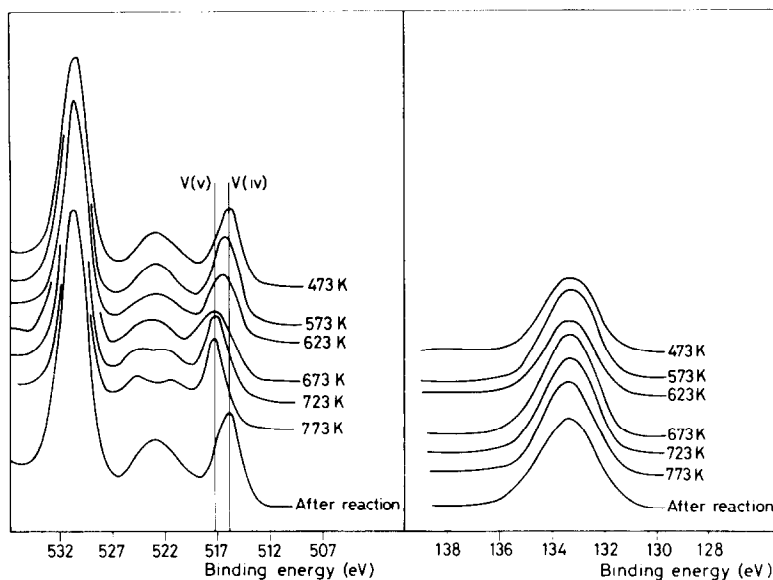
FIG. 6. O $1s$, V $2p$ (left), and P $2p$ (right) XPS photoemission peaks of sample 3 calcined at various temperatures.

in the experimental peak profile. It is very interesting to observe that oxidation occurs at higher temperature in the presence of excess of phosphorus. If one considers both binding energies and $(P/V)_s$ ratios, it is clear that the larger variations in the latter occur in correspondence with the oxidation process.

XPS results of discharged samples show a slight increase in $(P/V)_s$ values, though maintaining the same trend as that of dried samples (Fig. 5). Also the binding energies generally appear unchanged, with vanadium in the tetravalent state. The presence of V(V) was observed only for $(P/V)_b < 1$.

DISCUSSION

The role of the excess of phosphorus in (V,P)O catalysts for the oxidation of C_4 hydrocarbons to maleic anhydride has been widely discussed in the scientific literature. It is generally accepted (11, 15) that a slight excess of phosphorus (P/V atomic ratio from 1.05 to 1.1) is necessary for obtaining high catalytic performance. Due to the lack of selectivity data, the present catalytic results are rather preliminary. However, some important conclusions can still be drawn from the conversion data of the butane oxidation reaction. The specific (and also the overall) conversion increases by an order of magnitude for $(P/V)_b$ just exceeding unity (Fig. 4), in accordance with other studies (3).

Also the decrease of the specific conversion for higher $(P/V)_b$ values is not unexpected. The observed maximum has previously been correlated with a maximum in
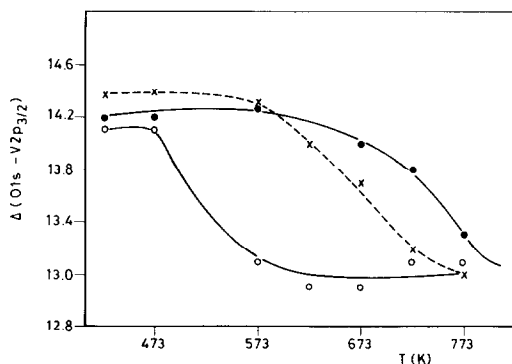

FIG. 7. Difference between O $1s$ and V $2p_{3/2}$ binding energies as a function of the calcination temperature: (○) sample 1; (●) sample 3; (×) sample 5.

SSA values and hydrogen reducibility of the catalyst (7). Thus, the ability of the catalyst to release oxygen in a non-selective way was assumed to determine the overall activity. In the present work, SSA does not seem to play an important role, since the experimental values are rather similar (Table 2). However, after reaction, vanadium still appeared as V(IV) in most catalysts, while the presence of V(V) was observed only for $(P/V)_b < 1$. This confirms that an easy oxidation of V(IV) is detrimental to the catalytic activity. The slow decrease of specific conversion for $(P/V)_b > 1$ is more difficult to understand. Although such a behavior has previously been observed (3, 7), the reported interpretations cannot strictly be applied in the present case because of different phase distributions in the catalysts and the well-known strong relation between catalytic behavior and occurrence of particular phases. However, the results seem to indicate that the aggregation state of vanadyl ions, embedded in a structure of phosphate ions, may play a key role in catalytic performance.

The EXAFS experiments reported here constitute one of the few measurements of the P K-absorption line, at least on catalyst samples. However, apart from an increase in structural disorder, no particular trends or variations in the bonding parameters (coordination geometry and interatomic distances) were observed as a function of $(P/V)_b$ ratio. The data are in line with the presence of a tetrahedral oxygen coordination around phosphorus. It is concluded that excess of phosphorus has no structural effects on the phosphorus coordination. EXAFS analysis of the K-absorption edge of vanadium in the same catalyst samples is in progress and should be more revealing as can also be expected of a XANES study.

It has been suggested that an excess of phosphorus prevents complete oxidation of V(IV) to V(V) during calcination in air and allows formation of the active β phase (6). Hodnett et al. (7) have observed a strong influence of the $(P/V)_b$ ratio on the nature of the final catalyst and its activity. They indicate that for low $(P/V)_b$ values β-VPO$_5$ (with V(V)) is obtained upon calcination, whereas for higher values a V(IV)-containing phase is formed, with a XRD diagram differing from that of the β phase. In this study such a phase has been observed but only in traces. It may be inferred that the composition of the calcined catalyst depends strongly on the nature of the reducing agent, namely HCl (6) or lactic acid (7). Such an influence on the solid-phase formation and catalytic behavior has also been established when using oxalic acid (4), hydrazine (5), or other organic acids (3).

This work shows clearly that excess of phosphorus delays oxidation of V(IV). From Fig. 6 it is evident that the temperature of oxidation is higher with increasing $(P/V)_b$.

The observation that $(P/V)_s$ increases with $(P/V)_b$ up to a plateau, occurring at a value slightly higher than unity, is in agreement with the results of Hodnett et al. (7). However, in our case such a relationship between the two variables was found only for dried samples. The behavior is different for catalyst calcined at 773 K (absence of the plateau). In order to explain this apparent disagreement we speculate that the oxidation number of vanadium has to be taken into account. The V(V)/V(IV) ratio of the samples of Ref. (7) is constant over the whole composition range, and the binding energy of vanadium appears unchanged by calcination. In our samples, oxidation occurs during calcination, and a connection is observed between the onset of oxidation and the largest variation of the $(P/V)_s$ ratio. Thus, it is the oxidation of vanadium which determines the different relationship between surface and bulk composition. This is confirmed if we consider the results obtained on samples after calcination at 673 K and catalytic reaction: vanadium remains tetravalent (for $(P/V)_b \geq 1$) and consequently the plateau is still present, even

though at a higher $(P/V)_s$ value. For all samples, the $(P/V)_s$ are rather higher (roughly about twice) than expected on the basis of bulk compositions. We have made a similar observation also for a different series of samples, both before and after calcination (5). However, in the latter case we observed a tendency to decrease after thermal treatment. Similar high values $(P/V = 2.4$ in the plateau region) were also found by Hodnett et al. (7), who argued that P acts as a diluent on the surface, isolating V ion sites and thus increasing the selectivity. Due to uncertainty in the XPS quantitative analysis, the authors did not further stress the point. In fact, since the sensitivity factors of V and P are 2.1 and 0.25, respectively, that is in the proportion 8 : 1, small errors in the intensity measurement for phosphorus or a mild matrix effect for the same element strongly affect the final result. However, as similar values are now being obtained in different laboratories for nonidentical series of catalysts, confidence increases that the results have a real basis.

ACKNOWLEDGMENTS

REFERENCES

1. Varma, R. L., and Saraf, D. N., *I&EC Prod. Res. Dev.* **18**, 7 (1979).
2. Budi, F., Neri, A., and Stefani, G., *Hydrocarbon Process.*, 159 (1982).
3. Nakamura, M., Kawai, K., and Fujiwara, Y., *J. Catal.* **34**, 345 (1974).
4. Poli, G., Resta, I., Ruggeri, O., and Trifirò, F., *Appl. Catal.* **1**, 393 (1981).
5. Garbassi, F., Bart, J. C. J., Montino, F., and Petrini, G., *Appl. Catal.* **16**, 271 (1985).
6. Centi, G., Galassi, C., Manenti, I., Riva, A., and Trifirò, F., *in* "Preparation of Catalysts, III" (G. Poncelet, P. Grange, and P. A. Jacobs, Eds.), p. 543. Elsevier, Amsterdam, 1983.
7. Hodnett, B. K., Permanne, P., and Delmon, B., *Appl. Catal.* **6**, 231 (1983); Hodnett, B. K., and Delmon, B., *Appl. Catal.* **9**, 203 (1984).
8. Lonsdale, K., Ed., *in* "International Tables for X-Ray Crystallography," Vol. III, p. 161. Kynoch Press, Birmingham, 1972.
9. Vlaic, G., and Bart, J. C. J., *Recl. Trav. Chim. Pays-Bas* **101**, 171 (1982).
10. Palmberg, P., *Anal. Chem.* **45**, 549A (1973).
11. Stefani, G., and Fontana, P. (to Lonza), U.S. Pat. 4 085 122 (1978).
12. Ladwig, G., *Z. Chem.* **8**, 307 (1968).
13. Bordes, E., and Courtine, P., *J. Catal.* **57**, 236 (1979).
14. Morselli, L., Riva, A., Trifirò, F., Zucchi, M., and Emig, G., *Chim. Ind. (Milan)* **60**, 791 (1978).
15. Mount, R. A., and Raffelson, H. (to Monsanto), U.S. Pat. Appl. B 330 394 (1975).